

Cyg OB2 #5: When three stars are just not enough.

M. Kennedy¹, S.M. Dougherty^{2,3}, P.M. Williams⁴ and A. Fink²

¹ University of Victoria, BC, Canada

² NRC-HIA DRAO, Penticton, BC, Canada

³ Institute for Space Imaging Science, University of Calgary, AB, Canada

⁴ Institute for Astronomy, Royal Observatory, Blackford Hill, Edinburgh, Scotland

Abstract: Archival observations from the Very Large Array (VLA) at frequencies between 1.4 GHz and 43 GHz of the 6.6-day O6.5-7+O5.5-6 binary Cyg OB2 #5 over 20 years are re-examined. The aim is to determine the location and character of its known variable radio emission. The radio emission consists of a primary component associated with the binary, and a non-thermal source (NE), 0.8'' to the NE. This work reveals that NE shows no evidence of variation demonstrating that the variable emission arises in the primary component. With NE constant, the radio flux from the primary can now be well determined for the first time, especially in observations that do not resolve both the primary and NE components. The variable radio emission from the primary has a period of 6.7 ± 0.3 years which is described by a simple model of a non-thermal source orbiting within the stellar wind envelope of the binary. Such a model implies the presence of a third, unresolved stellar companion (Star C) orbiting the 6.6-day binary with a period of 6.7 years. The non-thermal emission arises from either a WCR between Star C and the binary system, or possibly from Star C directly. Examination of radial velocity observations suggests reflex motion of the binary due to Star C, for which a mass of $23_{-14}^{+22} M_{\odot}$ is deduced. Together with the star associated with NE, this implies that Cyg OB2 #5 is a quadruple system.

1 Introduction

Cyg OB2 #5 (V729 Cyg, BD +40 4220) is an eclipsing binary system consisting of two O-type supergiants orbiting in a 6.6-day period (Hall, 1974; Leung & Schneider 1978; Rauw et al. 1999). This system is one of several luminous O-star systems in the Cyg OB2 association that shows evidence of variable radio emission (Persi et al. 1983, 1990; Bieging et al. 1989). The radio emission has two states: a low-flux state of ~ 2 mJy at 4.8 GHz where the spectral index is consistent with thermal emission from a stellar wind, and a high-flux state of ~ 8 mJy at 4.8 GHz, where the spectral index is flatter than in the low state. The variations appear to have a ~ 7 -year period (Miralles et al. 1994) and have been attributed to variable non-thermal emission from an expanding plasmon arising in the binary (Bieging et al. 1989; Persi et al. 1990; Miralles et al. 1994).

Observations by Abbott et al. (1981) with the VLA revealed a primary component associated with the binary and a second component (hereafter NE) $\sim 0.8''$ to the NE of the primary radio source. NE appears non-thermal and Contreras et al. (1997) argue it is the result of a wind-collision region (WCR) between the stellar wind of the binary and that of a B0-2 V star, 0.9'' from the binary to the NE (Contreras et al. 1997).

The previous analyses of the radio emission from Cyg OB2 #5 are based on observations from the Very Large Array (VLA), obtained in all the different configurations of the array. Hence, the observations may or may not resolve the emission from both the primary and NE components. In this work, all VLA archive

radio observations of Cyg OB2 #5 are re-examined to produce a consistently calibrated data set. This analysis accounts for changes in the resolution of the observations and presents a consistent treatment of the emission from both the primary and NE sources in each observation. For the first time, the nature and evolution of the emission of both the primary and NE are determined. Kennedy et al. (2010) provide a more complete description of the work highlighted here.

2 Observations

A total of 50 VLA observations of Cyg OB2 #5 obtained between 1983 and 2003 were extracted from the NRAO archive, re-calibrated and analysed. Examples of the resulting deconvolved images at 8.4 GHz are shown in Fig. 1.

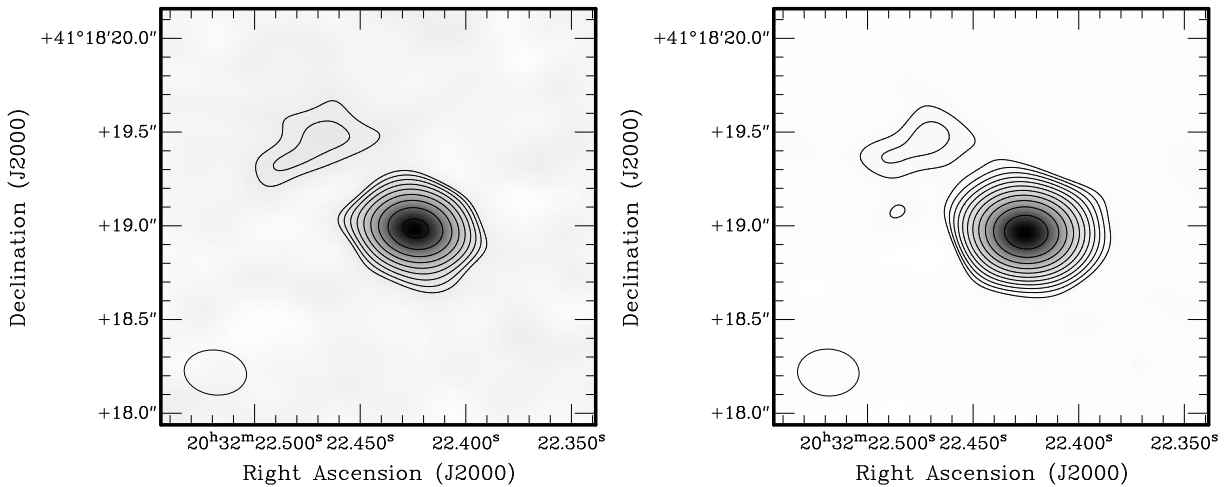


Figure 1: Two examples of the deconvolved VLA images at 8.4 GHz that show the primary and NE sources. The left image is from 1992 December 19 during a low emission state and the right image is from 1996 December 28 during a high emission state.

At 8.4 GHz, the two components were readily resolved in all observations obtained with A and B configuration of the VLA, whereas at 4.8 GHz the two components were only resolved in A-configuration observations. In all of these observations, NE was always detected. In C and D configurations, the two components are not resolved separately at any of the observing frequencies, with only a single unresolved source being observed. Higher resolution MERLIN observations at 1.4 GHz resolve the two radio components separately giving a 1.4-GHz flux for NE and confirming its non-thermal nature with a negative spectral index..

3 Analysis: variations in Radio Emission

The fluxes of Cyg OB2 #5 at both 4.8 GHz and 8.4 GHz as a function of time are shown in Fig. 2. Through the 20 years of observations it is evident that the 4.8-GHz emission from Cyg OB2 #5 has cycled through three cycles of high and low emission with an approximate period of ~ 7 yrs. It is also clear that the radio emission from NE shows no variation and the primary radio component is the source of the variations in Cyg OB2 #5.

At both 4.8 GHz and 8.4 GHz there were 12 and 11 epochs of VLA observations respectively where NE was resolved separately from the primary and a flux could be measured directly. These observations of NE have a weighted-mean flux at 4.8 GHz of 0.83 ± 0.11 mJy and 0.50 ± 0.12 mJy at 8.4 GHz. The flux of NE is statistically constant. This implies the variations arise exclusively in the primary radio source.

Knowing that NE is constant enables the flux of the primary to be determined for all observations where the two radio components are not spatially resolved. The period of the flux variations in the primary emission

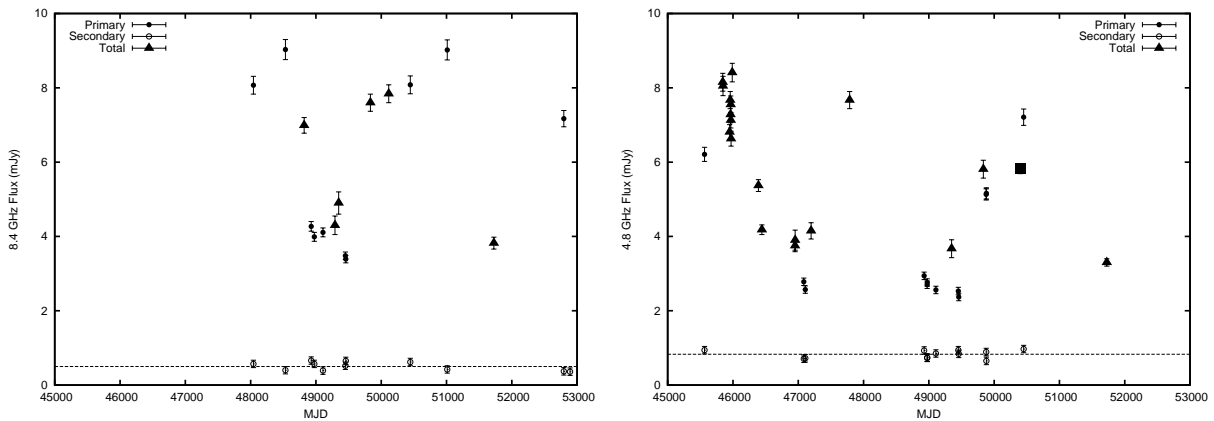


Figure 2: The fluxes of Cyg OB2 #5 between 1983 and 2003 at 8.4 GHz (left) and 4.8 GHz (right), with the primary (solid circles) and NE (open circles) and total i.e. when the components were *not* resolved as separate sources (solid triangles). The mean fluxes of NE are shown (dashed line). The MERLIN 4.8-GHz observation is shown as a square.

was determined using a string-length technique (van Loo et al. 2008, and references therein), and found to be 6.7 ± 0.3 years, remarkably similar to the “eyeball” period derived in previous works.

4 Discussion

4.1 The Primary and Variable Emission

The primary emission component is associated with the O-star binary system and is the source of all the observed variations in the radio emission. In the low state the primary radio emission is found to have a spectral index of 0.60 ± 0.04 , consistent with that expected for thermal emission arising in a steady-state radially symmetric stellar wind. The thermal emission must be reasonably constant since 350-GHz JCMT observations obtained away from radio minimum are consistent with the stellar wind spectrum deduced from the radio observations at radio minimum, with a best-fit spectral index 0.63 ± 0.04 across this broad frequency range.

During the high state, the spectral index is much flatter, with an index of 0.24 ± 0.01 . A model for the primary radio emission component is proposed, where the lower spectral index during high emission is the result of the addition of a non-thermal component to the thermal emission from the binary system that leads to a “composite” spectrum. Such a model has been successfully applied to describe the relatively flat continuum spectra of some Wolf-Rayet stars (e.g. Chapman et al., 1999) where the non-thermal emission arises in a WCR between the wind of the WR star and that of a massive companion star.

For a non-thermal source embedded in a thermal stellar wind plasma, the total observed flux as a function of frequency ν and at epoch t is the sum of the thermal and non-thermal fluxes, given by:

$$S_{obs}(\nu, t) = 2.5 \left(\frac{\nu}{4.8} \right)^{0.6} + S_{4.8}(t) \left(\frac{\nu}{4.8} \right)^{\alpha} e^{-\tau(\nu, t)} \quad \text{mJy},$$

where it is assumed the thermal emission component is constant with a spectral index of $+0.6$ and 4.8 GHz flux of 2.5 mJy measured in the low, thermal emission state, and $S_{4.8}(t)$ is the intrinsic 4.8-GHz flux of the non-thermal source at epoch t , α is the spectral index of the intrinsic non-thermal emission assumed to be constant. $\tau(\nu, t)$ is the line-of-sight free-free opacity through the stellar wind to the non-thermal source at frequency ν and epoch t , approximated by

$$\tau(\nu, t) \approx \tau_{4.8}(t) \left(\frac{\nu}{4.8} \right)^{-2.1}$$

where $\tau_{4.8}(t)$ is the 4.8-GHz line-of-sight free-free opacity at epoch t . The line-of-sight opacity is dependent on the geometry of the line-of-sight to the non-thermal emission. Here, the case of a non-thermal source in a 6.7-yr

orbit about the binary is considered. Williams et al. (1990) derived the varying free-free opacity along a line-of-sight to a non-thermal source orbiting in the circumbinary wind of the massive WR+O binary WR 140. The opacity is dependent on the orbit inclination (i), argument of periastron (ω), as well as the eccentric anomaly (e) and the time of periastron passage (T_0), hence

$$\tau_{4.8}(t) = \tau_{4.8}(t, i, \omega, e, T_0)$$

The intrinsic non-thermal flux $S_{4.8}(t)$ is expected to depend on the local conditions e.g. electron density, which will vary as the source moves through the dense circumbinary wind. This may be approximated by assuming a simple power-law relation with separation, namely

$$S_{4.8}(t) = S'_{4.8} r^{-s},$$

where $S'_{4.8}$ is the non-thermal flux when the separation is equal to a , and s is a power-law index. These definitions, along with the analytic form for $\tau_{4.8}(t)$ cf. Williams et al. 1990, allow $S_{obs}(\nu, t)$ to be determined as a function of the orbital phase of the non-thermal source orbiting the binary system. The resulting light curves arising from these models are plotted in Fig. 3 for four different model parameter sets, showing excellent agreement with the observations.

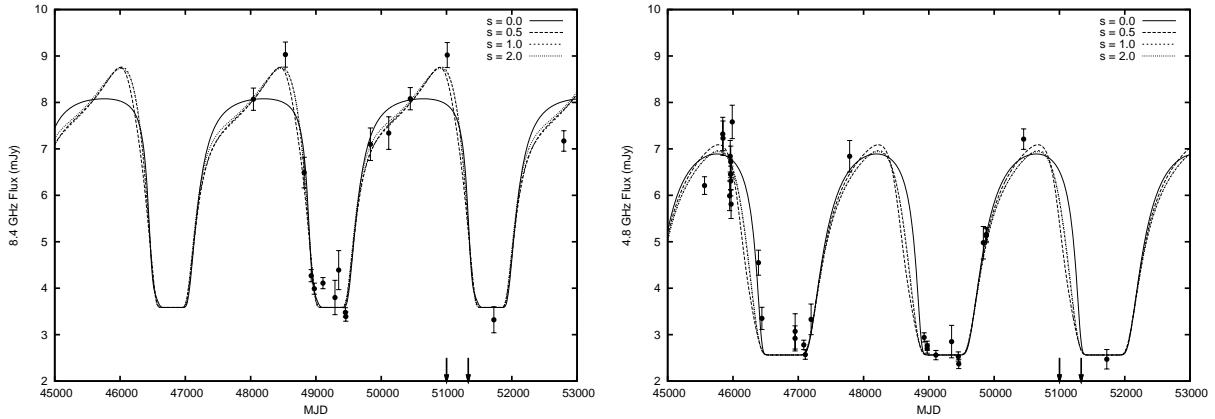


Figure 3: The best-fit orbiting non-thermal source model against the observed fluxes of the primary (slid circles) at 8.4 GHz (left) and 4.8 GHz (right) for the $s = 0, 0.5, 1$, and 2 models.

4.2 Evidence for a Third Star?

A non-thermal source orbiting the O+O binary system requires a star (hereafter Star C) to be in a 6.7-year orbit around the binary. This star may contribute the non-thermal radio emission via a WCR arising from the collision of its own stellar wind with the wind from the O+O star binary. Such WCRs have been observed directly in some WR+O star and O+O star binary systems (e.g. Dougherty & Pittard, 2006, and references therein). Alternatively, the non-thermal emission may arise from the putative third star directly, e.g. a compact object.

Given the high luminosities of the two supergiants in the binary and emission from circumstellar material, it will be very hard to detect the proposed third star directly, let alone measure its orbit. Instead, the radial velocities (RVs) of the O+O binary from Rauw et. al. (1999) and Bohannan & Conti (1976) are examined to search for reflex motion due to its putative orbit with Star C. For each RV observed from the primary, the residual (O–C) was calculated from the orbit by Rauw et. al. (1999) and formed the average (O–C) for each run. A systematic increase of RV between phases 0.26 and 0.89 is seen, implying that the O+O binary moves away from us more rapidly. This implies that Star C moves towards us more rapidly in this phase interval so that the circumbinary extinction to the non-thermal radio source diminishes, consistent with it brightening during this orbital phase.

The run of mean (O–C) with phase is compared with the reflex motion of the O+O binary in orbit with Star C following the orbital elements of the embedded non-thermal radio source from the $s = 0$ case (see Fig. 4). Fitting

$$v_r = \gamma + K_{\text{O+O}}(e \cos \omega + \cos(f + \omega))$$

for $K_{\text{O+O}}$ and systemic velocity γ , gives $K_{\text{O+O}} = 32 \pm 17 \text{ km s}^{-1}$ and $\gamma = -5.9 \pm 4.7 \text{ km s}^{-1}$. This leads to a mass function $f(m)$ derived from P (in days) and K (in km s^{-1}) from

$$f(m) = \frac{m_C^3 \sin^3(i)}{(m_{\text{O+O}} + m_C)^2} = 1.036 \times 10^{-7} (1 - e^2)^{3/2} K^3 P,$$

giving an estimate of the mass, m_C , of Star C. From the data here, $f(m) = 3.2_{-2.8}^{+8.2} M_\odot$. Assuming $\sin(i) = 1$ and adopting $m_{\text{O+O}} = 41.5 \pm 3.4 M_\odot$ from Linder et. al. (2009), this gives $m_C = 23_{-14}^{+22} M_\odot$ for Star C.

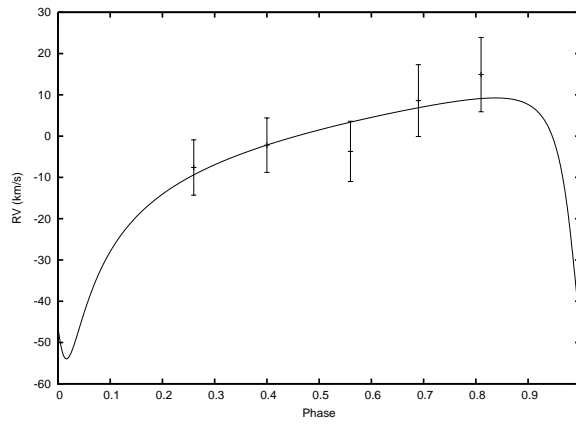


Figure 4: Observed (O–C) residuals and the RV curve for the reflex motion for the elements of the $s = 0$ model with $K = 32 \pm 17 \text{ km s}^{-1}$ and $\gamma = -5.9 \pm 4.7 \text{ km s}^{-1}$.

References

- Abbott, D. C., Biegging, J. H., & Churchwell, E. 1981, ApJ, 250, 645
 Biegging, J. H., Abbott, D. C., & Churchwell, E. B. 1989, ApJ, 340, 518
 Bohannan, B., & Conti, P. S. 1976, ApJ, 204, 797
 Chapman, J. M., Leitherer, C., Koribalski, B., Bouter, R., & Storey, M. 1999, ApJ, 518, 890
 Contreras, M. E., Rodriguez, L. F., Tapia, M., Cardini, D., Emanuele, A., Badiali, M., & Persi, P. 1997, ApJ, 488, L153
 Dougherty, S., & Pittard, J. M. 2006, in Proceedings of the 8th European VLBI Network Symposium
 Hall, D. S. 1974, Acta Astronomica, 24, 69
 Kennedy, M., Dougherty, S.M., Williams, P.M., Fink, A. 2010, ApJ, 709, 632
 Leung, K.-C., & Schneider, D. P. 1978, ApJ, 224, 565
 Linder, N., Rauw, G., Manfroid, J., Damerdji, Y., De Becker, M., Eenens, P., Royer, P., & Vreux, J.-M. 2009, A&A, 495, 231
 Miralles, M. P., Rodriguez, L. F., Tapia, M., Roth, M., Persi, P., Ferrari-Toniolo, M., & Curiel, S. 1994, A&A, 282, 547
 Persi, P., Ferrari-Toniolo, M., & Grasdalen, G. L. 1983, ApJ, 269, 625
 Persi, P., Ferrari-Toniolo, M., Tapia, M., Rodriguez, L. F., & Roth, M. 1990, A&A, 240, 93
 Rauw, G., Vreux, J.-M., & Bohannan, B. 1999, ApJ, 517, 416
 van Loo, S., Blomme, R., Dougherty, S. M., & Runacres, M. C. 2008, A&A, 483, 585
 Williams, P. M., van der Hucht, K. A., Pollock, A. M. T., Florkowski, D. R., van der Woerd, H., & Wamsteker, W. M. 1990, MNRAS, 243, 662